State-Constrained Bipartite Tracking of Interconnected Robotic Systems Via Hierarchical Prescribed-Performance Control

Ming-Feng Ge (gemf@cug.edu.cn)
China University of Geosciences https://orcid.org/0000-0002-6828-0147
Zhi-Wei Gu
China University of Geosciences
Peng Su
China University of Geosciences
Chang-Duo Liang
China University of Geosciences
Xiang Lu
Huazhong University of Science and Technology

Research Article

Keywords: State-constrained control, estimator based control, interconnected robotic systems (IRSs), prescribed performance

Posted Date: March 15th, 2022

DOI: https://doi.org/10.21203/rs.3.rs-1304630/v1

nonlinear dynamics manuscript No.
(will be inserted by the editor)

State-Constrained Bipartite Tracking of Interconnected Robotic Systems Via Hierarchical Prescribed-Performance Control

Ming-Feng Ge (✉) · Zhi-Wei Gu · Peng Su · Chang-Duo Liang · Xiang Lu

Received: date / Accepted: date

Abstract This paper investigates the collaborative design problem aiming to achieve state-constrained bipartite tracking of interconnected robotic systems (IRSs) with prescribed performance. We propose a hierarchical state-constrained estimator-based control frame to reduce the complexity of algorithms and improve the adaptation of the tracking control when the robotics are constrained to physical boundaries and external environment. Without the pre-known tracking trajectory, the estimator-based layer can estimate the tracking trajectory at each time interval by the interconnected topology. The position constraints are never violated during the convergence process by designing of control algorithms. The theoretical proof and simulation results are presented to validate the feasibility of the control algorithms.

Keywords state-constrained control · estimator-based control · interconnected robotic systems (IRSs) · prescribed performance

1 Introduction

In the last decades, the multi-agent systems were widely used in unmanned mobile vehicles, unmanned marine surface vehicles and unmanned air vehicles [1,2] due to the nice performance. Recently, the cooperative problems for networked robotic systems have become a academic hot spot due to it is highly autonomous, intelligent and flexible [3]-[5]. In practical application, the joint angles of robotics are limited by the complex working conditions and physical limits such that the output state of the robotics only occur within a certain range, i.e., the state of robotics is constrained. In the recent work, fault-tolerant output-constrained control in unknown Euler-Lagrange processes, tracking control with full-state constraint, and tracking control with constrained input and output have been studied [6]-[11]. Note that all the above-mentioned researches are concentrated on the single physical systems. However, it is difficult for a single individual to accomplish large and complex tasks efficiently. Therefore, there is still a lack a new type of control method for the interconnected robotic systems (IRSs) with state-constrained.

The cooperation problems for the IRSs have been researched recently. Nevertheless there may be non-cooperative individuals in practical applications, and it is common that the cooperation individuals and competition individuals participate in the same system simultaneously [12,13]. For example, in nature, the organisms cooperate with companions and compete other individuals to obtain abundant resources and benefits. In manufacturing, machines synchronously work on two opposite surfaces of the same workpiece to acquire the identical consequence. Based on above examples, the bipartite control problems containing cooperation and competition individuals are modeled by a signed graph [14], such as bipartite consensus [15], bipartite tracking [16,17] and bipartite formation [18], and the bipartite control problems are solved. The research on state-constrained bipartite tracking of the IRSs is still a blank.

Ming-Feng Ge (✉) · Zhi-Wei Gu · Peng Su · Chang-Duo Liang
School of Mechanical Engineering and Electronic Information, China University of Geosciences, Wuhan 430074, China
Xiang Lu
School of Chemistry and Chemical Engineering, Huazhong University of Science and Technology, Wuhan 430074, China

Corresponding author:Ming-Feng Ge
E-mail: gemf@cug.edu.cn

Recently, the control methods with prescribed performance have attracted great attention, and the prescribed performance control is used to guarantee the state errors of system stay in a prescribed region [19]-[22]. The tracking performance is an important index in the field of tracking control. In missile guidance and other tracking missions with accurate location, tracking control with prescribed performance is a necessary requirement. A adaptive sliding mode control with performance function is proposed in vehicular platoons [23]. A simple nonlogarithmic error mapping function guarantees that the errors of underwater vehicles are limited to a certain range [24]. However, all the above researches center on the single physical systems without interconnected individuals. The researches about prescribed performance control of the IRSs are scarce.

In this work, a hierarchical prescribed-performance control method is proposed such that the state-constrained bipartite tracking of the IRSs is achieved. The contributions of this paper mainly are following:

- Different from general researches considering state-constrained for single physical systems [25,26], the states of the robots are constrained in a range for the IRSs in convergence process in this paper. The output state of each robotic does not exceed the upper bound or low bound.
- In contrast with the common bipartite consensus problems [27,28], the bipartite tracking is applied in the IRSs and state constraints of the bipartite tracking are never violated during the state convergence concurrently.
- Compared with existing work of prescribed performance for multi-agent systems [29,30], a hierarchical control frame is used such that the tracking errors of the IRSs are limited to a prescribed range and the complexity and coupling of the IRSs are reduced in the whole control process.

The remaining parts are organized as follows. Section 2 provides the preliminaries including prerequisite knowledge and the problem formulations. In section 3, the state-constrained estimator-based control algorithm and its stability analysis are proposed. The simulation results are presented in section 4 to testify the effectiveness of the algorithm. Finally, the conclusions are summed up in section 5.

Notations	explanations
$\mathcal{R}^N$	$N \times 1$ real matrix
$\mathcal{R}^{N\times N}$	$N \times N$ real matrix
diag[·]	diagonal matrix
$I_{\rm n}$	n dimension identity matrix
max{·}	maximum values of the given vector
$\|\cdot\|$	the Euclidean norm
sgn(·)	the sign function
Z^+	Set of positive integer

2 Preliminaries

2.1 Graph theory

The communication of the IRSs can be modeled as a directed signed graph $\mathcal{G} = \{\mathcal{V}, \mathcal{E}, \mathcal{A}\}$, where $\mathcal{V} = \{1, 2, ..., N\}$ is the set of vertexes, $\mathcal{E} \subseteq \mathcal{V} \times \mathcal{V}$ is the set of edges, and $\mathcal{A} = [a_{ij}] \in \mathcal{R}^{N\times N}$ is the adjacency matrix. An edge $e_{ij} \in \mathcal{E}$ (i.e., $a_{ij} \neq 0$) implies that the mutual information flows directly from the vertex j to the vertex i, otherwise $a_{ij} = 0$. $a_{ij} > 0$ implies that the vertex i has the cooperative relationship with the vertex j, while $a_{ij} < 0$ implies that the vertex i has the competitive relationship with the vertex j. Furthermore, $\mathcal{G}$ is said to be a the strongly connected graph if there exists a path between any two vertexes. Assume that $\mathcal{G}$ has no self-loops, i.e., $a_{ii} = 0$. A cycle of $\mathcal{G}$ is denoted as the beginning and ending vertexes of the path being the same. Furthermore, a directed signed graph includes a directed spanning tree, and it implies that there is a rooted vertex which has a directed path to any other vertexes. The Laplacian matrix of the $\mathcal{G}$ is defined as $L_s = [l_{ij}] \in \mathcal{R}^{N\times N}$, where $l_{ii} = \sum_{j=1,j\neq i}^{N} |a_{ij}|$; $l_{ij} = -a_{ij}$, if $i \neq j$. A diagonal weighted matrix $B = \text{diag}[b_1, ..., b_N]$ represents the connection weight between the external agent and other agents. In detail, $b_i > 0$ implies that the i-th robotic can directly receive the information from the external robotic, otherwise $b_i = 0$.

Definition 1 *A directed signed graph is structurally balanced, if there exists two sets $\mathcal{V}_1$, $\mathcal{V}_2$ such that $\mathcal{V}_1 \cup \mathcal{V}_2 = \mathcal{V}$, $\mathcal{V}_1 \cap \mathcal{V}_2 = \emptyset$, where $a_{ij} > 0$ when the vertexes belong to the same set; $a_{ij} < 0$ when the vertexes belong to different sets.*

Assumption 1 *The directed signed graph is strongly connected and structurally balanced.*

2.2 System Specification

The IRSs are considered in the paper, which include N robotics connected by an interconnected network. The

model of the i-th robotic is described as follows

$$M_i(q_i)\ddot{q}_i + C_i(q_i,\dot{q}_i)\dot{q}_i + g_i(q_i) + d_i(t) = \tau_i, \tag{2.1}$$

where $t \geq 0$, $i \in \mathcal{V}$, $M_i(q_i) \in \mathcal{R}^{n\times n}$ represents the positive-definite inertia matrix, $q_i, \dot{q}_i, \ddot{q}_i \in \mathcal{R}^n$ are respectively the generalized position, velocity, and acceleration of the robotics, $C_i(q_i,\dot{q}_i) \in \mathcal{R}^{n\times n}$ stands for the centrifugal-Coriolis matrix, $g_i(q_i) \in \mathcal{R}^n$ represents the gravitational term, $d_i(t) \in \mathcal{R}^n$ is the input disturbance term satisfying $\sup_{t\geq 0}\|d_i(t)\| \leq d_M$, d_M is a positive constant, and $\tau_i \in \mathcal{R}^n$ denotes the control input to be designed subsequently for ensuring the state-constrained control.

To facilitate subsequent stability, (2.1) is remodeled as

$$\ddot{q}_i = {M_i}^{-1}(q_i)\tau_i - \chi_i, \tag{2.2}$$

where

$$\chi_i = {M_i}^{-1}(q_i)(C_i(q_i,\dot{q}_i)\dot{q}_i + g_i(q_i) + d_i(t)). \tag{2.3}$$

Property 1 The inertia matrix is a symmetric and positive definite matrix, and satisfies

$$x^T {M_i}^{-1}(q_i)x \geq m_1\|x\|^2,$$

where the constants m_1 is the minimum eigenvalue of ${M_i}^{-1}$.

On the other hand, the states of the leader including position q_0, velocity v_0 are proposed which satisfy the following equation $\dot{q}_0 = v_0$.

2.3 State Constraints and Decaying Functions

Due to the fact that most mechanical systems in applications are constrained to physical boundaries and external environment, we take the joint constraints of the mechanical systems into consideration, and propose a type of asymmetric time-varying state constraints of the IRSs, i.e.,

$$q_{lk}(t) < q_{ik}(t) < q_{uk}(t), k \in \{1,2,\ldots,n\}, \tag{2.4}$$

where $q_{ik}(t)$ is the k-th element of $q_i(t)$, $q_{lk}(t)$ and $q_{uk}(t)$ represent the lower bound and upper bound of the state constraints, respectively. A initial condition for ensuring (2.4) is

$$q_{lk}(0) < q_{ik}(0) < q_{uk}(0), k \in \{1,2,\ldots,n\}. \tag{2.5}$$

Assumption 2 *The boundary functions $q_{lk}(t)$, $q_{uk}(t)$ and their derivatives $\dot{q}_{lk}(t)$, $\dot{q}_{uk}(t)$ are bounded. In this way, there exist two constants a_l and a_u satisfying*

$$a_l \leq q_{uk}(t) - q_{lk}(t) \leq a_u. \tag{2.6}$$

Then, we provide a type of decaying functions with the following form

$$\zeta(\mathrm{t}) = (\zeta_0 - \zeta_\infty)e^{-\omega t} + \zeta_\infty, \tag{2.7}$$

where $\zeta_0 > 0$, $\omega > 0$ and $0 < \zeta_\infty < 1$ are preset parameters. It is obvious that $\zeta(\mathrm{t})$ monotonically decreases with the decreasing rate $e^{-\omega t}$ from 1 to the final value ζ_∞. Therefore, we give two decaying functions in order to restrain the position error and the velocity error respectively,

$$\zeta_1(\mathrm{t}) = (\zeta_{10} - \zeta_{1\infty})e^{-\omega_1 t} + \zeta_{1\infty}, \tag{2.8}$$
$$\zeta_2(\mathrm{t}) = (\zeta_{20} - \zeta_{2\infty})e^{-\omega_2 t} + \zeta_{2\infty}, \tag{2.9}$$

where the given parameters $\zeta_{10}, \zeta_{20}, \zeta_{1\infty}, \zeta_{2\infty}, \omega_1$ and ω_2 satisfy the above-mentioned rules.

Remark 1 The two decaying functions are devised to ensure that the position error and velocity error converge to the origin by a kind of exponential damping method, namely, each joint obeys the proposed asymmetric time-varying state constraints of the IRSs.

2.4 Problem Formulation

The bipartite tracking control of the IRSs is equal to the situation that position states $q_i(t)$ track the two opposite directions of target trajectory $q_0(t)$. For $i \in \mathcal{V}_1$, the position tracking error is defined as $e_i(t) = q_i(t) - q_0(t)$, while the velocity tracking error is defined as $\dot{e}_i(t) = v_i(t) - v_0(t)$, where $v_i(t) = \dot{q}_i(t)$. For $i \in \mathcal{V}_2$, the position tracking error is defined as $e_i(t) = q_i(t) + q_0(t)$, while the velocity tracking error is defined as $\dot{e}_i(t) = v_i(t) + v_0(t)$. The main control objective is to design the state-constrained estimator-based controller such that

- the followers track the target trajectory of the pilot agent with prescribed boundary, i.e., $\lim_{\mathrm{t}\to+\infty}\|e_i(t)\| < \delta_i, \forall i \in \mathcal{V}_1 \cup \mathcal{V}_2$, and δ_i is an selectable positive constant;
- the state constraints are never violated during state convergence, namely, $q_{lk}(t) < q_{ik}(t) < q_{uk}(t)$, $\forall k \in \{1,2,\ldots,n\}$, $\forall i \in \mathcal{V}_1 \cup \mathcal{V}_2$.

3 Main Results

3.1 Tracking Error Boundary

Before constructing the control algorithm, the tracking error transformation methods are developed. To obtain the prescribed performance, the decaying function is applied to the limits on the tracking error. Taking $i \in$

$\mathcal{V}_1$ as an example, the prescribed limits ρ_{uk} and ρ_{lk} are presented as follows

$$\begin{aligned}\rho_{uk} &= (q_{uk}(t) - q_{0k}(t))\zeta_1(t),\\ \rho_{lk} &= (q_{lk}(t) - q_{0k}(t))\zeta_1(t),\end{aligned} \tag{3.10}$$

where ρ_{lk} and ρ_{uk} are imposed to limit the error $e_i(t)$, q_{0k} is the k-th element of q_0. Based on Assumption 2 and the boundary of $q_{0k}(t)$, we could conclude that

$$q_{uk}(t) - q_{0k}(t) \leq a_u, q_{lk}(t) - q_{0k}(t) \geq -a_u. \tag{3.11}$$

It then follows from the property of the decaying function (8) and equation (10) that

$$\lim_{t\to+\infty} \rho_{uk} \leq \Delta_i, \lim_{t\to+\infty} \rho_{lk} \geq -\Delta_i, \tag{3.12}$$

where $\Delta_i = a_u\zeta_\infty$ is the tracking error boundary when the system is in the steady state. Similarly, when $i \in \mathcal{V}_2$, the tracking error boundary can be obtained by replacing q_{0k} with $-q_{0k}$.

3.2 State-Constrained Estimator-Based Control Algorithm

In this subsection, the state-constrained estimator-based control algorithm is proposed to solve the tracking problem of the IRSs with the state constraints.

Considering that not each robotic communicates with the target directly, a estimator algorithm is designed in a distributed way to estimate the states of the target such that each robotic acquires the states of the target in real time, which is presented as

$$\begin{cases}\dot{\hat{q}}_i = \alpha_1\left(\sum\limits_{j=1}^{N} a_{ij}(\hat{q}_j - \mathrm{sgn}(a_{ij})\hat{q}_i) + b_i(h_i q_0 - \hat{q}_i)\right) + \hat{v}_i,\\ \dot{\hat{v}}_i = \alpha_2 \mathrm{sgn}\left(\sum\limits_{j=1}^{N} a_{ij}(\hat{v}_j - \mathrm{sgn}(a_{ij})\hat{v}_i) + b_i(h_i v_0 - \hat{v}_i)\right),\end{cases} \tag{3.13}$$

where $\alpha_1, \alpha_2 > 0$ is the control gain, $\hat{q}_i$ and $\hat{q}_j$ are the estimated states of q_i and q_j, $\hat{v}_i$ and $\hat{v}_j$ are the estimated states of v_i and v_j. The estimator algorithm is able to render the estimated values $\hat{q}_i, \hat{v}_i$ tend to the leader states q_0, v_0 respectively.

Then, denote $\hat{e}_i = \hat{q}_i - h_i q_0$ and $\dot{\hat{\varepsilon}}_i = \hat{v}_i - h_i v_0$. We can further obtain that

$$\begin{cases}\dot{\hat{e}}_i = \alpha_1(\sum\limits_{j=1}^{N} a_{ij}(\hat{e}_j - \mathrm{sgn}(a_{ij})\hat{e}_i) - b_i\hat{e}_i) + \hat{\varepsilon}_i,\\ \dot{\hat{\varepsilon}}_i = \alpha_2 \mathrm{sgn}(\sum\limits_{j=1}^{N} a_{ij}(\hat{\varepsilon}_j - \mathrm{sgn}(a_{ij})\hat{\varepsilon}_i) - b_i\hat{\varepsilon}_i).\end{cases} \tag{3.14}$$

Furthermore, we establish the local control algorithm by the obtained estimated values $\hat{q}_i$ to track the trajectories of the leader finally.

For designing the controller of the local control layer, the local layer error is $\tilde{e}_i$=$q_i - \hat{q}_i$. $\tilde{e}_{ik}$ is the kth element of $\tilde{e}_i$, $k \in \{1, 2, \ldots, n\}$, which is the local layer error of each joint. The auxiliary virtual controller is prepared as follows

$$\beta_{ik}(t) = -c_i\varphi_{ik}(t), \tag{3.15}$$

$$\varphi_{ik}(t) = \ln(\frac{\tilde{e}_{ik}(t) - \rho_{lk}}{\rho_{uk} - \tilde{e}_{ik}(t)}), \tag{3.16}$$

where $c_i > 0$ represents the control gain, while $\varphi_{ik}(t)$ ensures $\rho_{lk} < \tilde{e}_{ik}(t) < \rho_{uk}$.

Moreover, the velocity error containing the virtual controller is presented as

$$\varepsilon_{ik}(t) = v_{ik}(t) - \beta_{ik}(t), \tag{3.17}$$

where $v_{ik} \in v_i$ is the velocity of the each joint. To achieve the stability of $\varepsilon_{ik}(t)$, the actual controller is designed by

$$\tau_i = -\lambda \left\|\varpi_i(t)\psi_i(t)\right\| \varpi_i(t)\psi_i(t). \tag{3.18}$$

where λ is the control gain, $\varpi_i(t) = \mathrm{diag}[\varpi_{i1}(t), \varpi_{i2}(t), ..., \varpi_{in}(t)]$, $\psi_i(t) = [\psi_{i1}(t), \psi_{i2}(t), ..., \psi_{in}(t)]^T$, and

$$\begin{aligned}\varpi_{ik} &= \frac{1}{\zeta_2}\sec^2(\frac{\pi\varepsilon_{ik}}{2\zeta_2}), k \in \{1, 2, \ldots, n\},\\ \psi_{ik}(t) &= tan(\frac{\pi\varepsilon_{ik}(t)}{2\zeta_2(t)}), k \in \{1, 2, \ldots, n\},\end{aligned} \tag{3.19}$$

where $|\varepsilon_{ik}(0)| < \zeta_2(0), i = 1, 2, ..., N$.

The general control frame for the state-constrained estimator-based control algorithm is presented in Fig. 1.

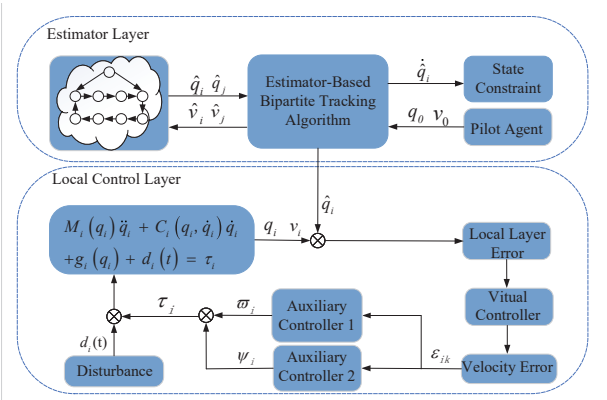

Fig. 1: The proposed hierarchical control frame.

Remark 2 Due to the fact that high nonlinearity, complex constructor and strong coupling, it is still difficult to solve the tracking control problem of IRSs with state constraints and prescribed performance. Therefore, we employ an estimator-based control algorithm to divide this complex problem into two simple problems. In detail, the estimator layer is designed to estimate the information of the pilot agent, while the estimated information can be transmitted to local control layer in time. Then, the local control layer applies the estimated values to achieve the control objective.

Remark 3 Considering the practical circumstance, the target trajectory is not a prior known information but a attainable information at each time instant. Therefore, the estimator layer render the information of the target trajectory transmit via a interconnected system at each time instant.

3.3 Stability Analysis for State-Constrained Estimator-Based Control Algorithm

Based on the designed control algorithm in Section 3.2, we need to ensure the stability of the estimator layer. Furthermore, the target trajectories at each time instant are acquired, while the boundedness of the convergence procedure can be guaranteed.

Theorem 1 *Suppose that Assumption 1 holds. By using the control algorithm (3.13), the bipartite tracking problem of the estimator layer can be solved, that is,* $\lim_{t\to+\infty}\|\hat{q}_i - q_0\| = 0$, $\forall i \in \mathcal{V}_1$ *and* $\lim_{t\to+\infty}\|\hat{q}_i + q_0\| = 0$, $\forall i \in \mathcal{V}_2$; $\lim_{t\to t_1}\|\hat{v}_i - v_0\| = 0$, $\forall i \in \mathcal{V}_1$ *and* $\lim_{t\to t_1}\|\hat{v}_i + v_0\| = 0$, $\forall i \in \mathcal{V}_2$.

Proof Based on (3.14), the compact form of the derivative of the velocity error is obtained that

$$\dot{\hat{\varepsilon}} = -\alpha_2 \mathrm{sgn}(((L_s + B) \otimes I_n)\hat{\varepsilon}). \tag{3.20}$$

For the convenience of proof, we define $\bar{\varepsilon} = (D \otimes I_n)\hat{\varepsilon}$. The velocity error can be transformed into $\dot{\bar{\varepsilon}} = -\alpha_2 \mathrm{sgn}((M_D \otimes I_n)\bar{\varepsilon})$, where $M_D = D(L_s + B)D$. From Lemma 3 in [31], if there exists a proper constant α_2 satisfying $\alpha_2 > \|\dot{v}_0\|$, $\bar{\varepsilon} \equiv 0$ as $t \geq t_1$, which is equal to $\hat{\varepsilon}_i \equiv 0$ as $t \geq t_1$, and t_1 can be calculated by [31]. Then, the results that $\lim_{t\to t_1}\|\hat{v}_i - v_0\| = 0$, $\forall i \in \mathcal{V}_1$ and $\lim_{t\to t_1}\|\hat{v}_i + v_0\| = 0$, $\forall i \in \mathcal{V}_2$ can be obtained.

Then, according to (3.14), the compact form of the derivative of the position error is obtained that

$$\dot{\hat{e}} = -\alpha_1((L_s + B) \otimes I_n)\hat{e} + \hat{\varepsilon}. \tag{3.21}$$

Due to the fact that $\hat{\varepsilon}_i \equiv 0$ as $t \geq t_1$, the position error can be transformed into $\dot{\bar{e}} = -\alpha_1((L_s + B) \otimes I_n)\hat{e}$ as $t \geq t_1$. Then, we define $\bar{e} = (D \otimes I_n)\hat{e}$. The compact form of the position error can be described as $\dot{\bar{e}} = -\alpha_1 \mathrm{sgn}((M_D \otimes I_n)\bar{e})$. From [32], if the graph $\mathcal{G}$ is heterogeneous and structurally balanced, then the matrix M_D is positive stable. Therefore, the system $\bar{e}$ is asymptotically stable. Obviously, the system $\hat{e}$ is also asymptotically stable. Then, we can conclude that $\lim_{t\to+\infty}\|\hat{e}_i\| = 0$, which is equal to the following two equations, $\lim_{t\to+\infty}\|\hat{q}_i - q_0\| = 0, \forall i \in \mathcal{V}_1$ and $\lim_{t\to+\infty}\|\hat{q}_i + q_0\| = 0, \forall i \in \mathcal{V}_2$.

Furthermore, the decaying rate of the position error $\hat{e}_i$ can be further acquired. The decaying rate can be described as the following equation

$$\forall t \geq t_1, \|\hat{e}_i(t)\| \leq \|\hat{e}_i(0)\| e^{-\mu t}, \tag{3.22}$$

where μ is a positive constant chosen in the simulation part.

Then, the two lemmas are given to demonstrate the Theorem 2.

Lemma 1 *For each agent* $i = 1, 2, ..., N$, *each joint* $k \in \{1, 2, \ldots, n\}$, *if*

$$\rho_{lk} < \tilde{e}_{ik}(t) < \rho_{uk} \tag{3.23}$$

is acquired, then the error $\tilde{e}_{ik}(t)$ *can be restricted in the boundary* $(-\Delta_i, \Delta_i)$ *with the decreasing rate* $e^{-\omega_1 t}$ *at last.*

Proof Because of the definition (3.10), we conclude that

$$q_{lk}(t) - q_{0k}(t) \leq \rho_{lk} < \rho_{uk} \leq q_{uk}(t) - q_{0k}(t).$$

Based on (3.11), it is obviously obtained that

$$0 \leq q_{uk}(t) - q_{0k}(t) \leq a_u,$$
$$-a_u \leq q_{lk}(t) - q_{0k}(t) < 0.$$

And it is further derived that

$$\rho_{uk} \leq a_u \zeta_1(\mathrm{t}),$$
$$\rho_{lk} \geq -a_u \zeta_1(\mathrm{t}).$$

Therefore, under the condition, the error satisfies that $|\tilde{e}_{ik}(t)| < a_u\zeta_1(\mathrm{t})$. Defining that Δ_i=$a_u\zeta_\infty$, the error will be limited in the constant set $(-\Delta_i, \Delta_i)$ ultimately. The proof is completed.

Before providing the proof, a variable is presented for the convenience, i.e.,

$$\sigma_i(t) = \frac{1}{(\tilde{e}_{ik}(t) - \rho_{lk})(\rho_{uk} - \tilde{e}_{ik}(t))}. \tag{3.24}$$

Lemma 2 *For each agent, if $\tilde{e}_{ik}(t)$, $\dot{\tilde{e}}_{ik}(t)$ and σ_i are bounded, so is $\dot{\beta}_{ik}(t)$.*

Proof Differentiating (3.15) by applying (3.24) yields

$$\begin{aligned}\dot{\beta}_{ik}(t) =& - c_i\sigma_i(t)((\rho_{uk}-\rho_{lk})\dot{\tilde{e}}_{ik}(t)\\ &+(\dot{\rho}_{lk}-\dot{\rho}_{uk})\tilde{e}_{ik}(t)+\dot{\rho}_{uk}\rho_{lk}-\dot{\rho}_{lk}\rho_{uk}).\end{aligned} \tag{3.25}$$

Based on the previous definitions and assumptions, the functions $\rho_{uk}, \rho_{lk}, \dot{\rho}_{uk}$, $\dot{\rho}_{lk} \in \mathcal{L}^{\infty}$. Therefore, $\dot{\beta}_{ik}(t)$ is bounded when $\tilde{e}_{ik}(t)$, $\dot{\tilde{e}}_{ik}(t)$ and σ_i are bounded. The proof is completed.

Theorem 2 *Considering the condition of initial values (2.5) and (3.19), the proposed actual controller can ensure the following inequations established.*

$$\rho_{lk} < \tilde{e}_{ik}(t) < \rho_{uk}, |\varepsilon_{ik}(t)| < \zeta_2(\mathrm{t}), k \in \{1,2,\ldots,n\}. \tag{3.26}$$

Proof The proof contains two steps including the stability of the position error and the velocity error. In addition, the position errors are demonstrated to keep stable in the constraint sets as the inequation (3.26).

In what follows, we apply the reduction to absurdity to prove the theorem. It is assumed that there exist time instants $t_v, v \in Z^+$ such that one or more of the following conditions found: $(1)\tilde{e}_{ik}(t_v) \geq \rho_{uk}(t_v); (2)\tilde{e}_{ik}(t_v) \leq \rho_{lk}(t_v); (3)\,|\varepsilon_{ik}(t_v)| \geq \zeta_2(t_v)$, where t_v is regarded as the first time to violate the restricted conditions. Therefore, for $0 < t < t_v$, $\rho_{lk} < \tilde{e}_{ik}(t) < \rho_{uk}$ and $|\varepsilon_{ik}(t)| < \zeta_2(\mathrm{t})$ hold.

Because of the continuity of the errors $\tilde{e}_{ik}$ and ε_{ik}, we can further conclude that one or more of the following limiting scenes hold: $(1)\lim\limits_{t\to t_v^-}\tilde{e}_{ik}(t_v) = \rho_{uk}(t_v); (2)\lim\limits_{t\to t_v^-}\tilde{e}_{ik}(t_v) = \rho_{lk}(t_v); (3)\lim\limits_{t\to t_v^-}|\varepsilon_{ik}(t)| = \zeta_2(t_v)$. The subsequent analysis will be presented to render the above inferences wrong.

Step 1: The position error is firstly considered. The Lyapunov function candidate is selected as follows

$$V_1 = \frac{1}{2}\varphi_{ik}^2. \tag{3.27}$$

Differentiate (3.27) with (3.15), it can be obtained that

$$\begin{aligned}\dot{V}_1 =& \varphi_{ik}\sigma_i((\rho_{uk}-\rho_{lk})\dot{\tilde{e}}_{ik}(t)+(\dot{\rho}_{lk}-\dot{\rho}_{uk})\tilde{e}_{ik}(t)\\ &+\dot{\rho}_{uk}\rho_{lk}-\dot{\rho}_{lk}\rho_{uk}).\end{aligned} \tag{3.28}$$

Due to the definition of $\tilde{e}_i$, one obtains that

$$\dot{\tilde{e}}_{ik}(t) = \varepsilon_{ik}(t) - c_i\varphi_{ik}(t) - \dot{\hat{q}}_{ik}(t). \tag{3.29}$$

By substituting (3.29) into the (3.28), we conclude that

$$\dot{V}_1 = \varphi_{ik}\sigma_i(\rho_{uk}-\rho_{lk})(\omega_i - c_i\varphi_{ik}),$$

$$\omega_i = (\varepsilon_{ik}(t) - \dot{\hat{q}}_{ik}(t) + \frac{\dot{\rho}_{lk}-\dot{\rho}_{uk}}{\rho_{uk}-\rho_{lk}}\tilde{e}_{ik}(t) + \frac{\dot{\rho}_{uk}\rho_{lk}-\dot{\rho}_{lk}\rho_{uk}}{\rho_{uk}-\rho_{lk}}).$$

In the following, we demonstrate the boundedness of ω_i during $t < t_v$. Under above-mentioned the boundedness of $\dot{q}_{lk}(t), \dot{q}_{uk}(t)$ and $\dot{\hat{q}}_i(t)$, we obtain that $\dot{\rho}_{lk} \in \mathcal{L}^{\infty}$, $\dot{\rho}_{uk} \in \mathcal{L}^{\infty}$. From (2.6) and (2.7), we get

$$a_l\zeta_{1\infty} < \rho_{uk}(t) - \rho_{lk}(t) < a_u,$$

which is equal to

$$\frac{1}{a_l\zeta_{1\infty}} < \frac{1}{\rho_{uk}(t)-\rho_{lk}(t)} < \frac{1}{a_u}.$$

Therefore, the boundedness of the ω_i is proved. There exists a constant o_i such that

$$|\omega_i| < o_i, t < t_v. \tag{3.30}$$

Based on (3.10) and(3.24), we obtain that

$$\sigma_i(\rho_{uk}-\rho_{lk}) > 0. \tag{3.31}$$

Considering (3.30) and (3.31), we attain

$$\dot{V}_1 \leq \sigma_i(\rho_{uk}-\rho_{lk})\,|\varphi_{ik}|\,(o_i - c_i\,|\varphi_{ik}|).$$

It is obvious that $\dot{V}_1 < 0$ as $|\varphi_{ik}| > \frac{o_i}{c_i}$. On account of (3.27), we conclude that $\dot{V}_1 < 0$ as $V_1 > \frac{o_i^2}{2c_i^2}$. Based on properties of the Lyapunov function and three hypothetical scenes, one has

$$\begin{aligned}&V_1(t) \leq \max\left\{V_1(0), \tfrac{o_i^2}{2c_i^2}\right\}, t < t_v,\\ &|\varphi_{ik}(t)| \leq \max\left\{\varphi_{ik}(0), \tfrac{o_i}{c_i}\right\}, t < t_v.\end{aligned} \tag{3.32}$$

By (3.32), there exists a contradictory deduction between the derived result and three hypothetical scenes. Therefore, the hypothesis that position errors violate the specified rules is invalid, i.e., the required result (3.26) is true.

Step 2: Then the velocity error is proved to satisfy the needs of dynamic behaviors. Select the Lyapunov function candidate as

$$V_2 = \frac{1}{\pi}\psi_i^T\psi_i. \tag{3.33}$$

The derivative of V_2 is

$$\dot{V}_2 = \frac{2}{\pi}\psi_i^T\dot{\psi}_i. \tag{3.34}$$

From (3.19), we derive $\dot{\psi}_{ik} = \frac{\pi}{2}\varpi_{ik}\left(\ddot{q}_{ik} - \dot{\beta}_{ik} - \frac{\varepsilon_{ik}\dot{\zeta}_2}{\zeta_2}\right)$. Furthermore,

$$\dot{\psi}_i = \frac{\pi}{2}\varpi_i\left(\ddot{q}_i - \dot{\beta}_i - \gamma\right), \tag{3.35}$$

where $\gamma = [\frac{\varepsilon_1\dot{\zeta}_2}{\zeta_2}, \frac{\varepsilon_2\dot{\zeta}_2}{\zeta_2}, ..., \frac{\varepsilon_n\dot{\zeta}_2}{\zeta_2}]^T$.

Substituting (2.2) into (3.35), one has

$$\dot{\psi}_i = \frac{\pi}{2}\varpi_i(\Gamma - \lambda \left\|\varpi_i(t)\psi_i(t)\right\| M_i^{-1}\varpi_i(t)\psi_i(t)), \quad (3.36)$$

$$\Gamma = -\chi_i - \dot{\beta}_i - \gamma, \quad (3.37)$$

where $\chi_i \in [\chi_1, \chi_2, ..., \chi_N]$, $\beta_i = [\beta_{i1}, \beta_{i2}, ..., \beta_{in}]$.

Inserting (3.36) into (3.33),

$$\begin{aligned}\dot{V}_2 =& \frac{2}{\pi}\psi_i^T\left(\frac{\pi}{2}\varpi_i(\Gamma - \lambda \left\|\varpi_i(t)\psi_i(t)\right\| M_i^{-1}\varpi_i(t)\psi_i(t))\right)\\ =&\psi_i^T\varpi_i(\Gamma - \lambda \left\|\varpi_i(t)\psi_i(t)\right\| M_i^{-1}\varpi_i(t)\psi_i(t))\\ \leq& \left\|\varpi_i\psi_i\right\|\left\|\Gamma\right\| - \lambda m_1 \left\|\varpi_i(t)\psi_i(t)\right\|\left\|\varpi_i(t)\psi_i(t)\right\|^2.\end{aligned} \quad (3.38)$$

Because of Property 1, we can obtain

$$-(\varpi_i\psi_i)^T M_i^{-1}(q_i)(\varpi_i\psi_i) \leq -m_1\|\varpi_i\psi_i\|^2 \quad (3.39)$$

for the above-mentioned inequation.

Then, the Lyapunov function is transformed into the following inequation

$$\dot{V}_2 \leq \left\|\varpi_i\psi_i\right\|\left(\left\|\Gamma\right\| - \lambda m_1\|\varpi_i(t)\psi_i(t)\|^2\right). \quad (3.40)$$

Subsequently, the boundedness of Γ is proved. Firstly, the boundedness of χ_i as $t < t_v$ is obtained by (2.3) on account of the boundedness of each system matrix. Based on Lemma 2, $\dot{\beta}_i \in \mathcal{L}^\infty$ as $t < t_v$ has been proved. Then, γ as $t < t_v$ is bounded on the basis of (3.17). Therefore, one has that there exists a positive constant κ such that

$$\left\|\Gamma\right\| \leq \kappa, t < t_v. \quad (3.41)$$

Furthermore,

$$\dot{V}_2 \leq \left\|\varpi_i\psi_i\right\|\left(\kappa - \lambda m_1\|\varpi_i(t)\psi_i(t)\|^2\right).$$

On the basis of the above analysis, we obtain $\dot{V}_2 < 0$ as $\left\|\varpi_i(t)\psi_i(t)\right\|^2 > \frac{\kappa}{\lambda m_1}$.

By means of (3.19), we conclude that

$$\begin{aligned}\left\|\varpi_i(t)\psi_i(t)\right\|^2 &= \sum_{i=1}^{n}\frac{\tan^2(\frac{\pi\varepsilon_{ik}(t)}{2\zeta_2(t)})}{\zeta_2^2(\mathrm{t})\cos^4(\frac{\pi\varepsilon_{ik}(t)}{2\zeta_2(t)})}\\ &\geq \sum_{i=1}^{n}\frac{\tan^2(\frac{\pi\varepsilon_{ik}(t)}{2\zeta_2(t)})}{\zeta_2^2(\mathrm{t})}\\ &\geq \sum_{i=1}^{n}\frac{\tan^2(\frac{\pi\varepsilon_{ik}(t)}{2\zeta_2(t)})}{\max\{\zeta_2^2\}} = \frac{\left\|\psi_i\right\|^2}{\max\{\zeta_2^2\}}.\end{aligned} \quad (3.42)$$

Furthermore, it is derived that $\dot{V}_2 < 0$ as $\left\|\psi_i\right\|^2 > \frac{\kappa}{\lambda m_1}\max\{\zeta_2^2\}$. Recalling (3.33), $V_2 \leq \frac{1}{\pi}\left\|\psi_i\right\|^2$. Therefore, $\dot{V}_2 < 0$ as $V_2 > \frac{\kappa}{\lambda\pi m_1}\max\{\zeta_2^2\}$. Based on properties of the Lyapunov function and three hypothetical scenes, it is derived that

$$\begin{aligned}&V_2(t) \leq \max\left\{V_2(0), \tfrac{\kappa}{\lambda\pi m_1}\max\{\zeta_2^2\}\right\}, t < t_v,\\ &\left\|\psi_i\right\| \leq \max\left\{\sqrt{\pi V_2(0)}, \sqrt{\tfrac{\kappa}{\lambda m_1}}\max\{\zeta_2\}\right\}, t < t_v.\end{aligned} \quad (3.43)$$

By (3.43), there exists a contradictory deduction between the derived result and three hypothetical scenes. Therefore, the hypothesis that velocity errors violate the specified rules is invalid, i.e., the required result (3.26) is true. Consequently, it is concluded that the proposed control algorithm could realize position and velocity states following the desired trajectories, while we ensure the state constraints effective simultaneously. According to Lemma 1, it is concluded that the proposed control algorithm can achieve bipartite tracking with prescribed performance successfully. The proof is completed.

Remark 4 Motivated by the above proof, the results of theorems can be further concluded that the tracking errors including local layer error and estimator layer are constrained in the boundary, that is,

$$\begin{aligned}\forall t \geq t_1, \|e_i\| &= \|\tilde{e}_i + \hat{e}_i\| \leq \|\tilde{e}_i\| + \|\hat{e}_i\|\\ &< \sqrt{n}a_u((\zeta_{10} - \zeta_{1\infty})e^{-\omega_1 t} + \zeta_{1\infty})\\ &+ \|\hat{e}_i(0)\|\, e^{-\mu t}.\end{aligned} \quad (3.44)$$

And $\lim_{t\to+\infty}\|e_i(t)\| = \sqrt{n}\Delta_i$, which satisfies the demand $\lim_{\mathrm{t}\to+\infty}\|e_i(t)\| < \delta_i$.

4 Simulation Results

In this subsection, several simulation examples are presented to testify the effectiveness of the control algorithm. The simulation parts can be divided into three parts including the estimator layer, the local control layer and the total control algorithm.

The estimator layer is applied to achieve the communication need of each agent. The communication topology includes one pilot agent and eight following agents. The eight following agents can be divided into two groups. In one group, four following agents cooperate with each other. In different groups, the following agents compete with each other. One pilot agent only transmit information to a fraction of following agents. And eight following agents are able to transmit information separately. The topology is displayed in Fig.1.

The control object of local control layer is to manipulate eight following agents to track the pilot agent. The single Euler-lagrange agent is described as two-link robot manipulator. The detailed physical parameters of

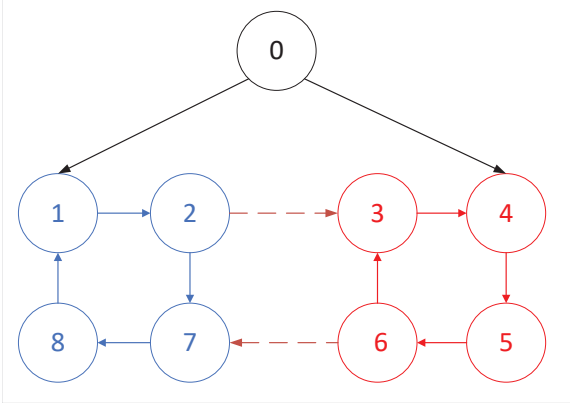

Fig. 2: The communication topology.

the eight following agents are listed in Table 1, where $m_{\Re}, \Re \in \{1, 2\}$ is the quality of the link, $l_{\Re}$ stands for the length of the link, $r_{\Re}$ is described as barycenter of the link and $J_{\Re}$ represents the moment of inertia of the link.

In the simulation part, the initial values of actual values and estimated values of position and velocity are given in a random way. The control objective is to track the trajectory of the the pilot agent. The tracking trajectories of position and velocity are given as follows

$$\begin{aligned} q_0 &= [sin(t) - \frac{t}{5}; sin(t) + \frac{t}{5}], \\ v_0 &= [cos(t) - \frac{1}{5}; cos(t) + \frac{1}{5}]. \end{aligned} \tag{4.45}$$

Besides, the position constraints of the joint rotation are supposed to obey the given limiting conditions as follows

$$\begin{aligned} -2 - \frac{t}{5} < q_i(t) < 2 - \frac{t}{5}, \forall i \in \mathcal{V}_1, \\ -2 + \frac{t}{5} < q_i(t) < 2 + \frac{t}{5}, \forall i \in \mathcal{V}_2. \end{aligned} \tag{4.46}$$

Furthermore, for the aforementioned controller, we choose the parameters as $\alpha_1 = 1$, $\alpha_2 = 2$, $c_i = 8$, $\kappa = 8$, $\mu = 0.25$ and $\lambda = 8$. Then, the decaying function for restraining the position errors and the velocity errors is selected as

$$\begin{aligned} \zeta_1(t) &= (1 - 0.01)\mathrm{e}^{-0.25t} + 0.01, \\ \zeta_2(t) &= (3 - 0.03)\mathrm{e}^{-0.25t} + 0.03. \end{aligned} \tag{4.47}$$

Employing the proposed control algorithm, we achieve the control objective of tracking the trajectory by two-link robot manipulators. The simulation graph Figs. 3-10 are presented to testify the effectiveness of the control frame and the control algorithms. The joint position states q_{i1} and q_{i2} can track the trajectories of the pilot agent, while the states are limited by the designed lower bounds q_{l1}, q_{l2} and upper bounds q_{u1} , q_{u2} (see Fig. 3). The estimated position states $\hat{q}_{i1}$ and $\hat{q}_{i2}$ can track the trajectories of the pilot agent(see Fig. 4). The velocity states v_{i1} and v_{i2} of each agent can track the velocity states of the pilot agent(see Fig. 5). Besides, the control frame is divided into the estimator layer and local control layer. The position tracking errors of the estimator layer and local control layer are also restricted in the prescribed boundary (see Figs. 6-7). In Fig. 6, the local control errors $\tilde{e}_{i1}$ and $\tilde{e}_{i2}$ are limited in the lower bounds ρ_{l1}, ρ_{l2} and upper bounds ρ_{u1}, ρ_{u2}. In Fig. 7, the estimator layer errors $\hat{e}_{i1}$ and $\hat{e}_{i2}$ are limited in the lower bound and upper bound. In Fig. 8, the local control errors $\dot{\tilde{e}}_{i1}$ and $\dot{\tilde{e}}_{i2}$ are presented. In Fig. 9, the estimator layer errors $\hat{\varepsilon}_{i1}$ and $\hat{\varepsilon}_{i2}$ are presented. Besides, the total tracking errors are also proposed to ensure the state-constrained control in the process of tracking in Fig. 10.

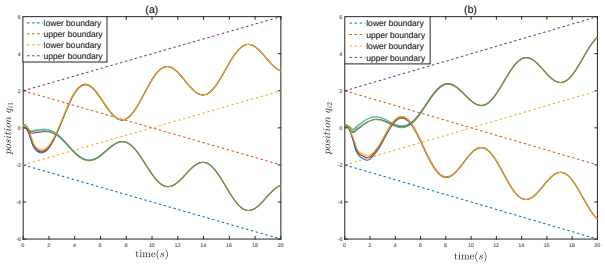

Fig. 3: Pictures (a) and (b) reveal the evolution of q_i for links 1 and 2 respectively.

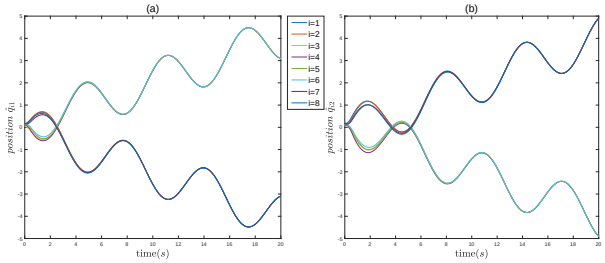

Fig. 4: Pictures (a) and (b) reveal the evolution of $\hat{q}_i$ for links 1 and 2 respectively.

5 Conclusion

This paper designs a new state-constrained estimator-based bipartite tracking algorithm for the IRSs with

Table 1: The physical parameters of two-link robot manipulators.

i-th robot	$m_{\Re}(kg)$	$l_{\Re}(m)$	$r_{\Re}(m)$	$J_{\Re}(kg \cdot m^2)$
1	1.32, 1.08	2.76, 2.48	1.38, 1.24	0.84, 0.55
2	1.23, 1.02	2.64, 2.42	1.32, 1.21	0.71, 0.50
3	1.26, 1.04	2.68, 2.44	1.34, 1.22	0.75, 0.52
4	1.32, 1.08	2.76, 2.48	1.38, 1.24	0.84, 0.55
5	1.23, 1.02	2.64, 2.42	1.32, 1.21	0.71, 0.50
6	1.26, 1.04	2.68, 2.44	1.34, 1.22	0.75, 0.52
7	1.32, 1.08	2.76, 2.48	1.38, 1.24	0.84, 0.55
8	1.23, 1.02	2.64, 2.42	1.32, 1.21	0.71, 0.50

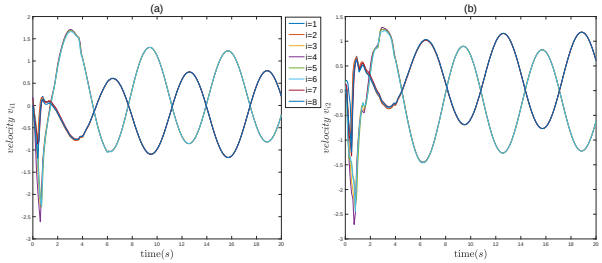

Fig. 5: Pictures (a) and (b) reveal the evolution of v_i for links 1 and 2 respectively.

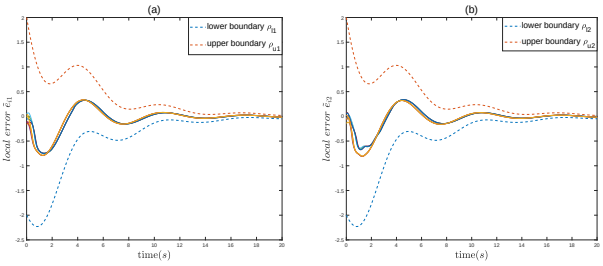

Fig. 6: Pictures (a) and (b) reveal the evolution of $\tilde{e}_i$ for links 1 and 2 respectively.

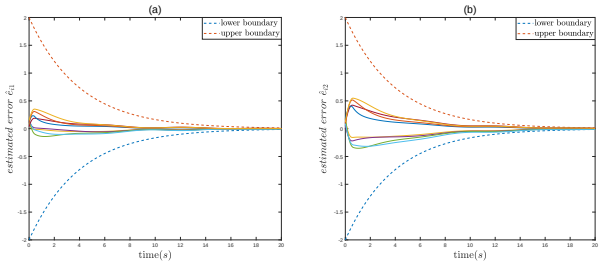

Fig. 7: Pictures (a) and (b) reveal the evolution of $\hat{e}_i$ for links 1 and 2 respectively.

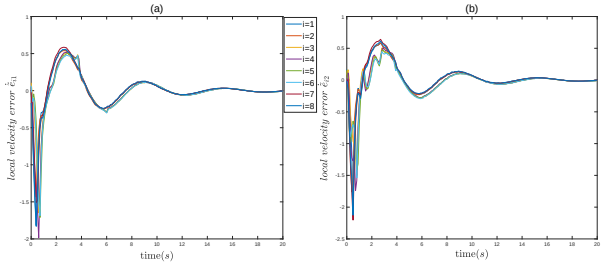

Fig. 8: Pictures (a) and (b) reveal the evolution of $\dot{\tilde{e}}_i$ for links 1 and 2 respectively.

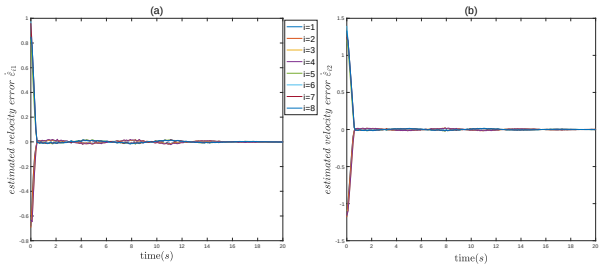

Fig. 9: Pictures (a) and (b) reveal the evolution of $\hat{\varepsilon}_i$ for links 1 and 2 respectively.

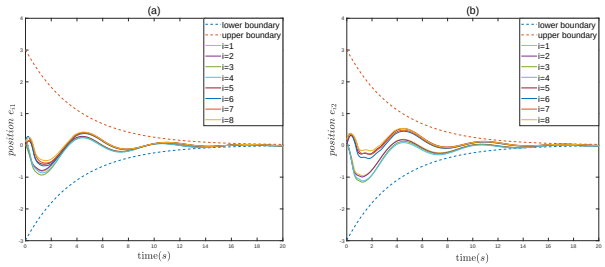

Fig. 10: Pictures (a) and (b) reveal the evolution of e_i for links 1 and 2 respectively.

prescribed performance and the constraint of position states. A new estimator-based control algorithm has good performance such that (1)the tracking problem with prescribed accuracy is achieved; (2)the position constraint is never violated during the convergence process;(3) the estimator-based control algorithm reduces complexity of algorithm without the pre-known tracking trajectory. The theoretical analysis and simulation results prove the effectiveness of the control algorithm. It is effortless to extend to formation tracking problem of networked complex systems and multi-target tracking problem of networked complex systems. The IRSs with both state-constrained condition and prescribed convergence time will be further studied.

Acknowledgements This work was supported by the National Key Technology R & D Program of China under Grants (2020YFB1709301, 2020YFB1709304), the Teaching Laboratory Open Fund Project, China University of Geosciences (Wuhan).

Compliance with ethical standards

Conflict of interest The authors declare that they have no conflict of interest.

Data availability statements Datas sharing is not applicable to this article as no datasets were generated or analyzed during the current study.

References

1. Zhang, Y., Mou, Z., Gao, F.:UAV-enabled secure communications by multi-agent deep reinforcement learning. IEEE Transactions on Vehicular Technology. 69(10), 11599-11611(2020)
2. Wu, F., Zhang, H., Wu, J.:Cellular UAV-to-device communications: Trajectory design and mode selection by multi-agent deep reinforcement learning. IEEE Transactions on Communications. 68(7), 4175-4189(2020)
3. Wang, H.:Task-space synchronization of networked robotic systems with uncertain kinematics and dynamics. IEEE Transactions on Automatic Control. 58(12), 3169-3174(2013)
4. Wang, H.:Passivity based synchronization for networked robotic systems with uncertain kinematics and dynamics. Automatica. 49(3), 755-761(2013)
5. Li, X., Wen, C., Chen, C.:Adaptive formation control of networked robotic systems with bearing-only measurements. IEEE Transactions on Cybernetics. 51(1), 199-209(2020)
6. Jin, X.:Fault tolerant finite-time leader-follower formation control for autonomous surface vessels with LOS range and angle constraints. Automatica. 68, 228-236(2016)
7. Jin, X.:Fault tolerant nonrepetitive trajectory tracking for MIMO output constrained nonlinear systems using iterative learning control. IEEE Transactions on Cybernetics. 49(8), 3180-3190(2018)
8. Liu, Y. J., Tong, S.:Barrier Lyapunov functions for Nussbaum gain adaptive control of full state constrained nonlinear systems. Automatica. 76, 143-152(2017)
9. Liu, Y. J., Lu, S., Tong, S., Chen, X., Chen, C. P., Li, D. J.:Adaptive control-based barrier Lyapunov functions for a class of stochastic nonlinear systems with full state constraints. Automatica. 87, 83-93(2018)
10. Xu, J. Z., Ge, M. F., Ling, G., Liu, F., Park, J. H.:Hierarchical predefined-time control of teleoperation systems with state and communication constraints. International Journal of Robust and Nonlinear Control. 31, 9652-9675(2021)
11. Zhang, J. X., Yang, G. H.:Fault-tolerant output-constrained control of unknown Euler-Lagrange systems with prescribed tracking accuracy. Automatica. 111, 108606(2020)
12. Tian, Z. P., Nie, R. X., Wang, J. Q., Long, R. Y.:Adaptive consensusbased model for heterogeneous large-scale group decision making: Detecting and managing non-cooperative behaviors. IEEE Transactions on Fuzzy Systems. 29(8), 2209-2223(2020)
13. Zhai, S. D., Zheng, W. X.:On survival of all agents in a network with cooperative and competitive interactions. IEEE Transactions on Automatic Control. 64(9), 3853-3860(2019)
14. Wen, G.,Wang, H., Yu, X., Yu, W.:Bipartite tracking consensus of linear multi-agent systems with a dynamic leader. IEEE Transactions on Circuits and Systems II: Express Briefs. 65(9), 1204-1208(2017)
15. Chen, Y., Zuo, Z., Wang, Y.:Bipartite consensus for a network of wave PDEs over a signed directed graph. Automatica. 129, 109640(2021)
16. Ding, T. F., Ge, M. F., Liu, Z. W.:Discrete-communication-based bipartite tracking of networked robotic systems via hierarchical hybrid control. IEEE Transactions on Circuits and Systems I: Regular Papers. 67(4), 1402-1412(2020)
17. Wu, Y. D., Ge, M. F., Ding, T. F.:Task-space bipartite tracking of networked robotic systems via hierarchical finite-time control. Nonlinear Dynamics. 100(4), 3469-3483(2020)
18. Yan, C. H., Zhang, W., Su, H. S., Li, X. H.:Adaptive bipartite time-carying output formation control for multiagent systems on signed directed graphs. IEEE Transactions on Cybernetics.
19. Bechlioulis, C. P., Rovithakis, G. A.:Robust adaptive control of feedback linearizable MIMO nonlinear systems with prescribed performance. IEEE Transactions on Automatic Control. 53(9), 2090-2099(2008)
20. Bechlioulis, C. P., Rovithakis, G. A.:A low-complexity global approximation-free control scheme with prescribed performance for unknown pure feedback systems. Automatica. 50(4), 1217-1226(2014)
21. Theodorakopoulos, A., Rovithakis, G. A.:Low-complexity prescribed performance control of uncertain MIMO feedback linearizable systems. IEEE Transactions on Automatic Control. 61(7), 1946-1952(2015)
22. Wang, W., Wen, C.:Adaptive actuator failure compensation control of uncertain nonlinear systems with guaranteed transient performance. Automatica. 46(12), 2082-2091(2010)
23. Guo, G., Li, D.:Adaptive sliding mode control of vehicular platoons with prescribed tracking performance. IEEE Transactions on Vehicular Technology. 68(8), 7511-7520(2019)
24. Li, J., Du, J., Sun, Y., Lewis, F. L.:Robust adaptive trajectory tracking control of underactuated autonomous underwater vehicles with prescribed performance. International Journal of Robust and Nonlinear Control. 29(14), 4629-4643(2019)
25. Xu, Z. B., Xie, N. G., Shen, H., Hu, X. L., Liu Q. Y.:Extended state observer-based adaptive prescribed

performance control for a class of nonlinear systems with full-state constraints and uncertainties. Nonlinear Dynamics. 105, 345-358(2021)
26. Yao, Y. G., Tan, J. Q., Wu, J., Zhang, X.:Event-triggered fixed-time adaptive fuzzy control for state-constrained stochastic nonlinear systems without feasibility conditions. Nonlinear Dynamics. 105, 403-416(2021)
27. Zhang, T. Z., Li, H. Y., Liu. J., Lu, D. W., Xie, S. R., Luo, J.:Distributed multiple-bipartite consensus in networked Lagrangian systems with cooperative-competitive interactions. Nonlinear Dynamics. 106(3), 2229-2244(2021)
28. Zhao, L. Y., Ji, J.C., Li, W., Bai. M. H.:Weighted bipartite containment motion of Lagrangian systems with impulsive cooperative-competitive interactions. Nonlinear Dynamics. 104, 2417-2431(2021)
29. Li, X. L., Luo, X. Y., Wang, J. G., Guan, X. P.:Finite-time consensus of nonlinear multi-agent system with prescribed performance. Nonlinear Dynamics. 91(4), 2397-2409(2018)
30. Liu, D. C., Liu, Z., Philip Chen, C. L., Zhang, Y.:Distributed adaptive fuzzy control approach for prescribed-time containment of uncertain nonlinear multi-agent systems with unknown hysteresis. Nonlinear Dynamics. 105(1), 257-275(2021)
31. Yao, X. Y., Ding, H. F., Ge, M. F.:Task-space tracking control of multi-robot systems with disturbances and uncertainties rejection capability. Nonlinear Dynamics. 92(4), 1649-1664(2018)
32. Hu, J. P., Wu, Y., Liu, L., Feng, G.:Adaptive bipartite consensus control of high-order multiagent systems on coopetition networks. International Journal of Robust and Nonlinear Control. 28(7), 2868-2886(2018).